

Causal Inference for Continuous Multiple Time Point Interventions

Michael Schomaker^{1,2,3}

Helen McIlleron^{4,5}

Paolo Denti⁴

Iván Díaz⁶

Abstract

There are limited options to estimate the treatment effects of variables which are continuous and measured at multiple time points, particularly if the true dose-response curve should be estimated as closely as possible. However, these situations may be of relevance: in pharmacology, one may be interested in how outcomes of people living with -and treated for- HIV, such as viral failure, would vary for time-varying interventions such as different drug concentration trajectories. A challenge for doing causal inference with continuous interventions is that the positivity assumption is typically violated. To address positivity violations, we develop projection functions, which reweigh and redefine the estimand of interest based on functions of the conditional support for the respective interventions. With these functions, we obtain the desired dose-response curve in areas of enough support, and otherwise a meaningful estimand that does not require the positivity assumption. We develop g -computation type plug-in estimators for this case. Those are contrasted with g -computation estimators which are applied to continuous interventions without specifically addressing positivity violations, which we propose to be presented with diagnostics. The ideas are illustrated with longitudinal data from HIV positive children treated with an efavirenz-based regimen as part of the CHAPAS-3 trial, which enrolled children < 13 years in Zambia/Uganda. Simulations show in which situations a standard g -computation approach is appropriate, and in which it leads to bias and how the proposed weighted estimation approach then recovers the alternative estimand of interest.

1 Introduction

Causal inference for multiple time-point interventions has received considerable attention in the literature over the past few years: if the intervention of interest is binary, popular estimation approaches include inverse probability of treatment weighting approaches (IPTW) [1], g -computation estimators [2, 3] and longitudinal targeted maximum likelihood estimators (LTMLE) [4], among others. For IPTW, the treatment and censoring mechanisms need to be estimated at each time point, parametric g -computation requires fitting of both the outcome and confounder mechanisms, sequential g -computation is based on the iterated outcome regressions only, and LTMLE needs models for the outcome, censoring, and treatment mechanisms, iteratively at each point in time. All of those methods are relatively well-understood and have been successfully applied in different fields (e.g., in [5–10]).

However, suggestions on how to estimate treatment effects of variables that are continuous and measured at multiple time points are limited. This may, however, be of interest to construct causal dose-response curves (CDRC). For example, in pharmacoepidemiology, one may be interested in how counterfactual outcomes vary for different dosing strategies for a particular drug, see Section 2.

Early work on continuous interventions includes the seminal paper of Robins, Hernán and Brumback [1] on inverse probability weighting of marginal structural models (MSMs). For a single time point, this requires the estimation of stabilized weights based on the conditional density of the treatment, given the confounders. This density may be estimated with parametric regression models, such as linear regression models. The MSM, describing the dose-response relationship (i.e., the CDRC), can then be obtained using weighted regression. The suggested approach can also be used for the longitudinal case, where

¹Department of Statistics, Ludwig-Maximilians University, Munich, Germany, michael.schomaker@stat.uni-muenchen.de

²Centre for Infectious Disease Epidemiology and Research, University of Cape Town, Cape Town, South Africa

³Institute of Public Health, Medical Decision Making and Health Technology Assessment, UMIT – University for Health Sciences, Medical Informatics and Technology, Hall in Tirol, Austria

⁴Division of Clinical Pharmacology, Department of Medicine, University of Cape Town, South Africa

⁵Wellcome Centre for Infectious Diseases Research in Africa (CIDRI-Africa), Institute of Infectious Disease and Molecular Medicine, University of Cape Town, Cape Town, South Africa

⁶Division of Biostatistics, Department of Population Health, New York University Grossman School of Medicine; New York, United States of America

stabilized weights can be constructed easily, and one may work with a working model where, for example, the effect of cumulative dose over all time points on the response is estimated.

There are several other suggestions for the point treatment case (i.e., a single time point): for example, the use of the generalized propensity score (GPS) is often advocated in the literature [11]. Similar to the MSM approach described above, both the conditional density of the treatment, given the confounders, and the dose-response relationship have to be specified and estimated. Instead of using stabilized weights, the GPS is included in the dose-response model as a covariate. To reduce the risk of bias due to model mis-specification, it has been suggested to incorporate machine learning (ML) in the estimation process [12]. However, when combining GPS and ML approaches, there is no guarantee for valid inference, i.e., related confidence intervals may not achieve nominal coverage [4]. Doubly robust (DR) approaches allow the integration of ML while retaining valid inference. As such, the DR-estimator proposed by Kennedy et al. [13] is a viable alternative to both MSM and GPS approaches. It does not rely on the correct specification of parametric models and can incorporate general machine learning approaches. As with other, similar, approaches [14] both the treatment and outcome mechanisms need to be modelled. Then a pseudo-outcome based on those two estimated nuisance functions is constructed, and put into relationship with the continuous intervention using kernel smoothing. Further angles in the point treatment case are given in the literature [15–18].

There are fewer suggestions as to how to estimate CDRCs for multiple time point interventions. As indicated above, one could work with inverse probability weighting of marginal structural models and specify a parametric dose-response curve. Alternatively, one may favour the definition of the causal parameter as a projection of the true CDRC onto a specified working model [19]. Both approaches have the disadvantage that, with mis-specification of the dose-response relationship or an inappropriate working model, the postulated curve may be far away from the true CDRC. Moreover, the threat of practical positivity violations is even more severe in the longitudinal setup, and working with inverse densities – which can be volatile – remains a serious concern [20]. It has thus been suggested in the literature to avoid these issues by changing the scientific question of interest, if meaningful, and to work with alternative definitions of causal effects.

For example, Young et al. [21] consider so-called modified treatment policies, where treatment effects are allowed to be stochastic and depend on the natural value of treatment, defined as the treatment value that would have been observed at time t , had the intervention been discontinued right before t . A similar approach relates to using representative interventions, which are stochastic interventions that maintain a continuous treatment within a pre-specified range [22]. Diaz et al. [23] present four estimators for longitudinal modified treatment policies (LMTPs), based on IPTW, g-computation and doubly robust considerations. These estimators are implemented in an R-package (`lmtp`). An advantage of those approaches is that the usual positivity assumption can be substantially relaxed. Moreover, the proposed framework is very general, applicable to longitudinal and survival settings, and one is not forced to make arbitrary parametric assumptions if the doubly robust estimators are employed. It also avoids estimation of conditional densities as it recasts the problem at hand as a classification procedure for the density ratio of the post-intervention and natural treatment densities. A disadvantage of the approach is that it does not aim at estimating the CDRC, which may, however, relate to the research question of interest, see Section 2 below.

In this paper, we are interested in counterfactual outcomes after intervening on a continuous intervention (such as drug concentration) at multiple time points. For example, we may be interested in the probability of viral suppression after one year of follow-up, had HIV-positive children had a fixed concentration level of efavirenz during this year. In this example, it would be desirable to estimate the true CDRC as closely as possible, to understand and visualize the underlying biological mechanism and decide what preferred target concentrations should be. This comes with several challenges: most importantly, violations of the positivity assumption are to be expected with continuous multiple time-point interventions. If this is the case, estimands that are related to modified treatment policies or stochastic interventions, as discussed above, would elegantly tackle the positivity violation problem, but redefine the question of interest. In pharmacoepidemiology and other fields this may be not ideal, as interpretations of the true CDRC are of considerable clinical interest, for example to determine appropriate drug target concentrations.

We suggest a g-computation based approach to estimate and visualize (weighted) causal dose-response curves. The proposed approach computes counterfactual outcomes for multiple values of the continuous intervention (at each time point). We then define regions of low support through low values of the conditional treatment density, evaluated at the intervention trajectories of interest. Our proposal is to redefine the estimand of interest only in those regions, based on suitable projection functions. Such an approach entails a compromise between identifiability and interpretability; that is, the tradeoff one has to make is between estimating the CDRC as closely as possible, at the risk of bias due to positivity violations and minimizing the risk of bias due to positivity violations, at the cost of redefining the estimand (e.g. by using modified treatment policies). Our paper explores both the case where one attempts to estimate the CDRC as closely as possible and situations in which a compromise may be acceptable, if positivity violations are of major concern.

We introduce the motivating question in Section 2, followed by the theoretical framework in Section 3. After presenting our extensive Monte-Carlo simulations (Section 4), we analyze the illustrative data example in Section 5. We conclude in Section 6.

2 Motivating Example

Our motivating data example comes from *CHAPAS-3*, an open-label, parallel-group, randomised trial (CHAPAS-3) [24]. Children with HIV (aged 1 month to 13 years), from four different treatment centres (one in Zambia, three in Uganda) were assigned to receive antiretroviral therapy (ART) with fixed-dose combination tablets: random allocation related to the nucleoside reverse transcriptase inhibitors (NRTIs) abacavir, stavudine or zidovudine (i.e. the first drug), which was given together with lamivudine (second drug) and the third drug, a nonnucleoside reverse transcriptase inhibitor, either nevirapine or efavirenz (NNRTI, third drug, chosen at discretion of the treating physician). The primary endpoint were adverse events, both clinical (grade 2/3/4) and laboratory (confirmed grade 3, or any grade 4).

Several substudies of the trial explored pharmacokinetic aspects of the nonnucleoside reverse transcriptase inhibitors (i.e. efavirenz and nevirapine), in particular the relationship between the respective drug concentrations and elevated viral load, i.e. viral failure [25, 26]. In those studies, individual pharmacokinetic (PK) measures such as plasma concentration 12 hours after dose were determined through population PK modeling and associations with viral failure were explored using the Cox proportional hazards model, showing lower levels of failure with increased drug concentrations. The reason to focus on the concentration of the NNRTI drugs is because i) they are expected to be responsible for most of the viral suppression and ii) the action of NRTI drugs is intercellularly, which means that the measured plasma concentrations are not necessarily relevant.

As highlighted in similar studies [27–29], a refined hypothesis relates to understanding the biologic mechanism between drug concentration and viral outcomes: to determine optimal target concentrations that can be translated into recommended doses, possibly depending on patients’ metabolizing status. This equates to asking about the causal effect of drug concentration, measured and controlled over a particular time period, on viral failure. Understanding the true (nonlinear) intervention-outcome relationship is crucial as both too low and too high concentrations could result in negative outcomes. However, drawing a particular CDRC is challenging for the following reasons: (i) the form of the curve should be flexible and as close as possible to the truth; (ii) there exist time-dependent confounders (e.g., adherence, weight) that are themselves affected by prior concentration levels, making regression an invalid method for causal effect estimation [30]; (iii) with long follow-up and moderate sample size, positivity violations are an issue of concern that have to be addressed.

We illustrate our concepts using the data from Bienczak et al. [25]. More details on the data analysis are given in Section 5.

3 Framework

3.1 Notation

We consider a longitudinal data setup where at each time point t , $t = 0, 1, \dots, T$, we measure the outcome Y_t , a continuous intervention A_t and covariates L_t^j , $j = 1, \dots, q$. We denote $\mathbf{L}_0 = \{L_0^1, \dots, L_0^{q_0}\}$ as “baseline variables” and $\mathbf{L}_t = \{L_t^1, \dots, L_t^q\}$ as follow-up variables, with $q, q_0 \in \mathbb{N}$. The intervention and covariate histories of a unit i (up to and including time t) are $\bar{A}_{t,i} = (A_{0,i}, \dots, A_{t,i})$ and $\bar{L}_{t,i}^s = (L_{0,i}^s, \dots, L_{t,i}^s)$, $s = 1, \dots, q$, $i = 1, \dots, n$, respectively. The observed data structure is

$$O = (\mathbf{L}_0, A_0, Y_0, \mathbf{L}_1, A_1, Y_1, \dots, \mathbf{L}_T, A_T, Y_T) \stackrel{iid}{\sim} P_0.$$

We are interested in the counterfactual outcome $Y_{t,i}^{\bar{a}_t}$ that would have been observed at time t if unit i had received, possibly contrary to the fact, the intervention history $\bar{A}_{t,i} = \bar{a}_t$, $a_{t,i} \in \mathbb{R}$. For a given intervention $\bar{A}_{t,i} = \bar{a}_t$, the counterfactual covariates are denoted as $\bar{\mathbf{L}}_{t,i}^{\bar{a}_t}$. We use \mathbf{H}_t to denote the history of all data up to before A_t .

3.2 Estimands

3.2.1 Estimands for one time point

In order to illustrate the ideas, we first consider a simple example with only one time point where $O = (\mathbf{L}, A, Y)$. Assume \mathbf{L} has density $p_0(\mathbf{l})$ with respect to some dominating measure $\nu(\mathbf{l})$. In this case, the general dose-response curve $m : a \mapsto E(Y^a)$ can be identified [13] as

$$\begin{aligned} m(a) &= E_{\mathbf{L}}[E(Y^a \mid A = a, \mathbf{L})] = E_{\mathbf{L}}[E(Y \mid A = a, \mathbf{L})] \\ &= \int E(Y \mid A = a, \mathbf{L} = \mathbf{l}) p_0(\mathbf{l}) d\nu(\mathbf{l}), \end{aligned} \tag{1}$$

where the first equality follows by the law of iterated expectation and the assumption that Y^a is independent of A conditional on \mathbf{L} (conditional exchangeability), and the second one because $Y^a = Y$ in the event of $A = a$ (consistency).

An example of such a curve for a particular interval $[a_{\min}, a_{\max}]$ is given in Figure 1a.

This quantity is undefined if the conditional density function $g(a \mid \mathbf{l})$ is such that $\inf_{a \in \mathcal{A}} g(a \mid \mathbf{l}) = 0$ for values \mathbf{l} where $p_0(\mathbf{l}) > 0$ and \mathcal{A} denotes the set of all possible interventions $A = a$. Thus, it is usually required that $\inf_{a \in \mathcal{A}} g(a \mid \mathbf{l}) > 0$ almost everywhere, the so-called (strong) *positivity assumption*. In this paper, we address violations of the positivity assumption through a redefinition of the estimand of interest, where we replace the marginal distribution function of \mathbf{L} in (1) by a user-given distribution function. That is, we instead estimate

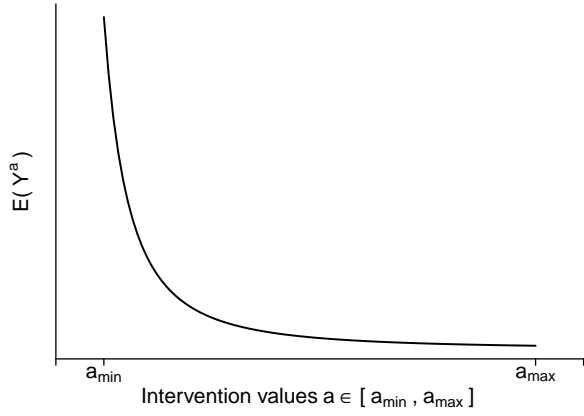
$$m_w(a) = \int E(Y \mid A = a, \mathbf{L} = \mathbf{l}) w(a, \mathbf{l}) p_0(\mathbf{l}) d\nu(\mathbf{l}) \tag{2}$$

for some weight function $w(a, \mathbf{l})$. To illustrate the construction of this function, consider two extreme cases: $w(a, \mathbf{l}) = 1$, and $w(a, \mathbf{l}) = g(a \mid \mathbf{l})/g(a)$, where $g(a)$ is the marginal density of A . Under the first case, we have $m_w(a) = m(a)$, which is equal to the dose-response curve whenever the positivity assumption holds. Under $w(a, \mathbf{l}) = g(a \mid \mathbf{l})/g(a)$, we have $m_w(a) = E(Y \mid A = a)$, which is not a causal quantity (unless exchangeability is assumed) but it does not require the positivity assumption. We therefore propose to use a function $w(a, \mathbf{l})$ such that $w(a, \mathbf{l}) \rightarrow 1$ in areas of \mathcal{A} that have good support, and $w(a, \mathbf{l}) \rightarrow g(a \mid \mathbf{l})/g(a)$ in areas of \mathcal{A} such that $g(a \mid \mathbf{l})$ is close to zero. Thus, one possible function to use is

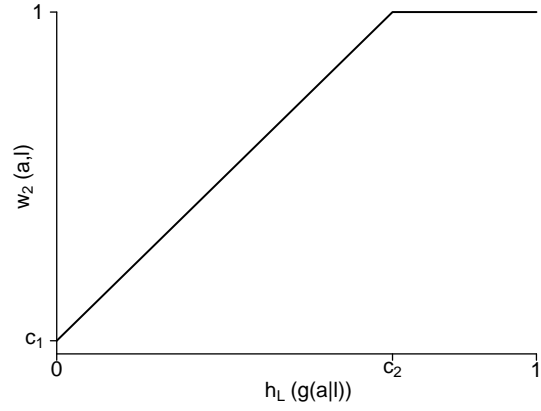
$$w_1(a, \mathbf{l}) = \begin{cases} 1 & \text{if } g(a \mid \mathbf{l}) > c \\ \frac{g(a \mid \mathbf{l})}{g(a)} & \text{otherwise.} \end{cases} \tag{3}$$

Using (3) yields the desired dose-response curve under enough support, and otherwise $E(Y \mid A = a)$. Note that both $m(a)$ and $m_w(a)$ are undefined outside the support region of A . For instance, in the

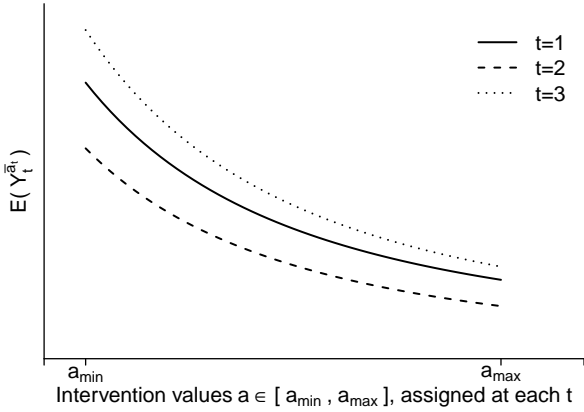
motivating data example the CDRC is undefined for negative concentration values and biologically implausible concentration values of > 40 mg/L.



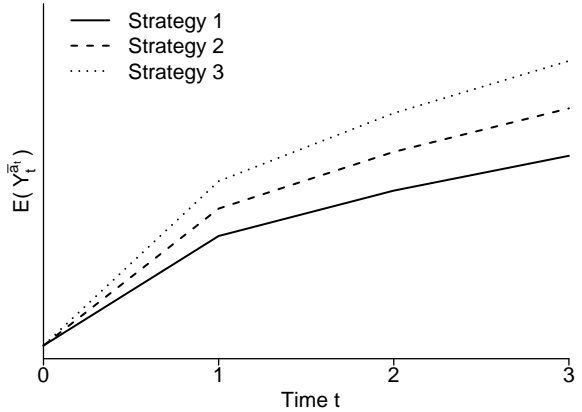
(a) CDRC for one time point



(b) Linear weight function



(c) Possible CDRC visualization
– if intervention values are constant over time



(d) Possible CDRC visualization
– if intervention values vary over time (or for survival data)

Figure 1: Considerations for causal dose-response curves (CDRCs)

Estimands under different weight functions

There are alternative weight functions that assign a weight of 1 under enough support, i.e when values of functions of $g(a, \mathbf{l})$ are large enough, and assign weights based on some density of A and/or \mathbf{L} otherwise:

$$w(a, \mathbf{l}) = \begin{cases} 1 & \text{if } h_1(g(a|\mathbf{l})) > c, \\ h_2(g(a, \mathbf{l})) & \text{if } h_1(g(a|\mathbf{l})) \leq c. \end{cases}$$

For example, consider the following weight choice which is illustrated in Figure 1b:

$$w_2(a, \mathbf{l}) = \begin{cases} 1 & \text{for } h_1(g(a | \mathbf{l})) > c_2 \\ c_1 + \frac{1-c_1}{c_2} \times h_2(g(a | \mathbf{l})) & \text{for } h_1(g(a | \mathbf{l})) \leq c_2 \end{cases} . \quad (4)$$

An interesting choice for both h_1 and h_2 is the expectation (function) with respect to \mathbf{L} : with this choice, we achieve that if the marginal support with respect to a is not large enough, the marginal support itself is used as the weight function. Such a weight choice has been motivated in the context of estimands that are defined through parameters in a marginal structural working model for (continuous summaries of) longitudinal binary interventions [31]. Then, for any $0 \leq c_1, c_2 \leq 1$, the estimand entails a

compromise between the CDRC and a weighted CDRC, weighted by *marginal* support for the respective interventions: for the latter, greater weight is given to interventions with greater marginal support; and the more support there is for each possible intervention choice, the estimand will be closer to the CDRC. This entails a pragmatic compromise between identifiability and interpretability. A similar tradeoff is achieved by using other weight choices that are monotone with respect to the density function $g(a | \mathbf{l})$, for example

$$w_3(a, \mathbf{l}) = \begin{cases} 1 & \text{if } g(a | \mathbf{l}) > c_2 \\ \frac{g(a|\mathbf{l})}{g(a|\mathbf{l})+c_1g(a)} & \text{if } g(a | \mathbf{l}) \leq c_2 \end{cases}, \quad w_4(a, \mathbf{l}) = \begin{cases} 1 & \text{if } g(a | \mathbf{l}) > c_2 \\ 1 - \exp \left\{ -c_1 \frac{g(a|\mathbf{l})}{g(a)} \right\} & \text{if } g(a | \mathbf{l}) \leq c_2 \end{cases}.$$

3.2.2 Estimands for Multiple Time Points

If there are multiple time points, we may typically be interested in how the counterfactual outcome at time t would change for all possible (or a set of selected) intervention trajectories – possibly conditional on some baseline variables. That is, we seek to estimate the causal dose-response curve

$$m_t : \bar{a}_t \mapsto E(Y_t^{\bar{a}_t} | \mathbf{L}_0^*) \quad \forall t \in \mathcal{T} \text{ and } \mathbf{L}_0^* \subseteq \mathbf{L}_0, \quad (5)$$

where $\mathcal{T} = \{0, 1, \dots, T\}$, $\bar{a}_t \in \bar{\mathcal{A}}_t$, and $\bar{\mathcal{A}}_t$ denotes either i) the set of all strategies $\bar{a}_t = (a_0, \dots, a_t)$ for which the curve is defined or ii) a relevant subset of interest. If we are interested in (5), we can identify the estimand through the sequential g-formula (also known as the iterated conditional expectation representation [3]) under sequential conditional exchangeability, consistency and positivity [32] as follows (we use $\mathbf{L}_0^* = \emptyset$ for ease of illustration):

$$\mathbb{E}(Y_t^{\bar{a}_t}) = \mathbb{E}(\dots \mathbb{E}(\mathbb{E}(Y_t | \bar{A}_t = \bar{a}_t, \bar{\mathbf{L}}_t) | \bar{A}_{t-1} = \bar{a}_{t-1}, \bar{\mathbf{L}}_{t-1}) \dots | A_0 = a_0, \mathbf{L}_0)). \quad (6)$$

In the above expression \bar{Y}_{t-1} is part of $\bar{\mathbf{L}}_t$. Because A_t is continuous, positivity requires that for the respective conditional density functions, we have $P(g(a_t | \mathbf{H}_t)) > 0 \quad \forall t$. More formally, we require

$$\inf_{a_t \in \mathcal{A}_t} g(a_t | \mathbf{h}_t) > 0 \quad \text{whenever} \quad p_0(\mathbf{l}_t | A_{t-1} = a_{t-1}, \mathbf{H}_{t-1} = \mathbf{h}_{t-1}) > 0 \quad \forall t \in \mathcal{T}. \quad (7)$$

This assumption may be relaxed under additional parametric modeling assumptions and the set \mathcal{A}_t may be reduced based on the scientific question of interest; see Section 3.3.2 for a thorough discussion. Consistency in the multiple time-point case is the requirement that $Y_t^{\bar{a}_t} = Y_t$ if $\bar{A}_t = \bar{a}_t$ and $\bar{\mathbf{L}}_t^{\bar{a}_t} = \bar{\mathbf{L}}_t$ if $\bar{A}_{t-1} = \bar{a}_{t-1}$. With sequential conditional exchangeability we require the counterfactual outcome under the assigned treatment trajectory to be independent of the actually assigned treatment at time t , given the past: $Y_t^{\bar{a}_t} \perp\!\!\!\perp A_t | \bar{H}_t$ for $t = 0, \dots, T$.

To link the above longitudinal g-computation formula to our proposals for one time point, it may be written in terms of the following recursion. Let $\tilde{m}_{t+1} = Y_t$. For $s = t, \dots, 0$ recursively define

$$\tilde{m}_s : (a_s, \mathbf{h}_s) \mapsto \int \tilde{m}_{s+1}(a_{s+1}, \mathbf{h}_{s+1}) dP_0(\mathbf{l}_{s+1} | A_s = a_s, \mathbf{H}_s = \mathbf{h}_s), \quad (8)$$

where $\int \tilde{m}_{s+1}(a_{s+1}, \mathbf{h}_{s+1}) dP_0(\mathbf{l}_{s+1} | A_s = a_s, \mathbf{H}_s = \mathbf{h}_s) = E(\tilde{m}_{s+1}(a_{s+1}, \mathbf{H}_{s+1}) | A_s = a_s, \mathbf{H}_s = \mathbf{h}_s)$.

Then, the counterfactual mean outcome $E(Y_t^{\bar{a}_t})$ is identified as $\mathbb{E}(\tilde{m}_0(A_0, H_0))$, which follows from the re-expression of (8) in terms of (6) by recursively evaluating the integral. The above recursive integral is well defined only if the positivity assumption (7) is met. As before, we propose to address violations of the positivity assumption by estimating the following quantity instead:

$$\tilde{m}_{w,s} : (a_s, \mathbf{h}_s) \mapsto \int \tilde{m}_{s+1}(a_{s+1}, \mathbf{h}_{s+1}) w_s(a_{s+1}, \mathbf{h}_{s+1}) dP_0(\mathbf{l}_{s+1} | A_s = a_s, \mathbf{H}_s = \mathbf{h}_s). \quad (9)$$

As before, if the weight function $w_s(a_{s+1}, \mathbf{h}_{s+1})$ is equal to one, the above expression can be used to define the actual CDRC (5) through recursive evaluation of (9). If, however, the weight function is equal to

$$w_s(a_{s+1}, \mathbf{h}_{s+1}) = \frac{g_s(a_{s+1} | \mathbf{h}_{s+1})}{g_s(a_{s+1} | a_s, \mathbf{h}_s)}, \quad (10)$$

then the estimand becomes

$$\tilde{m}_{w,s} : (a_s, \mathbf{h}_s) \mapsto \int \tilde{m}_{s+1}(a_{s+1}, \mathbf{h}_{s+1}) dP_0(\mathbf{l}_{s+1} \mid A_{s+1} = a_{s+1}, A_s = a_s, \mathbf{H}_s = \mathbf{h}_s) \quad (11)$$

by application of Bayes' rule. Intuitively, the above quantity does not remove confounding of the relation between A_{s+1} and Y_{s+1} , because it conditions on $A_{s+1} = a_{s+1}$ rather than fixing (i.e., intervening on) $A_{s+1} = a_{s+1}$. However, the above expression does not require the positivity assumption to be well defined, as motivated further below.

For the longitudinal case, we follow a strategy similar to that considered for the single time-point case, and consider a compromise between satisfying the positivity assumption and adjusting for confounding. This compromise can be achieved by using weight functions that are 1 in areas of good support, and are equal to (10) in areas of poor support. If the denominator in (10) is very small, we may want to compromise further:

$$w_{s,1}(a_{s+1}, \mathbf{h}_{s+1}, c) = \begin{cases} 1 & \text{if } g_s(a_{s+1} \mid \mathbf{h}_{s+1}) > c, \\ \frac{g_s(a_{s+1} \mid \mathbf{h}_{s+1})}{g_s(a_{s+1} \mid a_s, \mathbf{h}_s)} & \text{if } g_s(a_{s+1} \mid \mathbf{h}_{s+1}) \leq c \text{ and } g_s(a_{s+1} \mid a_s, \mathbf{h}_s) > c, \\ \frac{g_s(a_{s+1} \mid \mathbf{h}_{s+1})}{g_s(a_{s+1} \mid a_{s-1}, \mathbf{h}_{s-1})} & \text{if } g_s(a_{s+1} \mid \mathbf{h}_{s+1}) \leq c \text{ and } g_s(a_{s+1} \mid a_s, \mathbf{h}_s) \leq c \\ & \text{and } g_s(a_{s+1} \mid a_{s-1}, \mathbf{h}_{s-1}) > c, \\ \vdots & \vdots \\ \frac{g_s(a_{s+1} \mid \mathbf{h}_{s+1})}{g_s(a_{s+1})} & \text{otherwise .} \end{cases} \quad (12)$$

Using the weights (12) in (9) returns the CDRC if there is enough conditional support in terms of $g_s(a_{s+1} \mid \mathbf{h}_{s+1}) > c$ for all s ; if there is not enough conditional support and the weight denominator $g_s(a_{s+1} \mid a_s, \mathbf{h}_s)$ is greater than c for all time points, then the estimand equates to $E(Y_t \mid A_t = a_t, \dots, A_0 = a_0)$; this follows from recursively applying (11) for $s = t, \dots, 0$. Thus, no positivity assumption as defined in (7) is required for identification because whenever a positivity violation is present in terms of $g_s(a_{s+1} \mid \mathbf{h}_{s+1}) \leq c$ for a given a_{s+1} and \mathbf{h}_{s+1} (that is, either a structural violation or a practical violation at estimation stage) the weights (12) redefine the estimand in a way such that the assumption is not needed. Note that, as in the single time point case, the CDRC is undefined outside the support region of \bar{A}_t . If there is not enough conditional support and the weight denominator is smaller than c , the estimand entails an additional compromise. A different compromise is achieved if the weights are applied only at selected time points: the estimand then implies conditioning on $A_s = a_s$ for those time points, but intervening with $A_s = a_s$ on the others. However, it is difficult to think of situations where such an estimand would be meaningful.

The weighted CDRC can be interpreted as follows: those units which have a covariate trajectory that makes the intervention value of interest at t not unlikely to occur (under the desired intervention before t), receive the intervention at t ; all other units get different interventions that produce, on average, outcomes as we would expect among those who actually follow the intervention trajectory of interest (if the denominator $g_t(a_{t+1} \mid a_t, \mathbf{h}_t)$ is well-defined). Informally speaking, we calculate the CDRC in regions of enough support and make use of the marginal associations otherwise, if possible.

If we now reexpress our target quantity (9) in terms of an iterated conditional expectation representation, we get:

$$\mathbb{E}_{w_1}(Y_t^{\bar{a}_t}) = \mathbb{E}_{w_{1,0}}(\dots \mathbb{E}_{w_{1,t-1}}(\mathbb{E}_{w_{1,t}}(Y_t \mid \bar{A}_t = \bar{a}_t, \bar{\mathbf{L}}_t) \mid \bar{A}_{t-1} = \bar{a}_{t-1}, \bar{\mathbf{L}}_{t-1}) \dots \mid A_0 = a_0, \mathbf{L}_0), \quad (13)$$

where we define $\mathbb{E}_{w_{1,t}}(Y_t \mid \bar{A}_t = \bar{a}_t, \bar{\mathbf{L}}_t) = \mathbb{E}(w_{1,t} Y_t \mid \bar{A}_t = \bar{a}_t, \bar{\mathbf{L}}_t)$. This can be rewritten as

$$\mathbb{E}_{w_1}(Y_t^{\bar{a}_t}) = \int_{\bar{\mathbf{l}} \in \bar{\mathbf{L}}_t} \left\{ \frac{\mathbb{E}(w_{1,t} Y_t \mid \bar{\mathbf{A}}_t = \bar{a}_t, \bar{\mathbf{L}}_t = \bar{\mathbf{l}}_t) \times \prod_{r=0}^t f(\mathbf{l}_r \mid \bar{\mathbf{A}}_{r-1} = \bar{a}_{r-1}, \bar{\mathbf{L}}_{r-1} = \bar{\mathbf{l}}_{r-1})}{\prod_{r=0}^t f(\mathbf{l}_r \mid \bar{\mathbf{A}}_{r-1} = \bar{a}_{r-1}, \bar{\mathbf{L}}_{r-1} = \bar{\mathbf{l}}_{r-1})} \right\} d\bar{\mathbf{l}}, \quad (14)$$

where the second term in (14) is

$$\prod_{s=1}^{q-1} f(l_r^s | \bar{\mathbf{A}}_{r-1} = \bar{a}_{r-1}, \bar{\mathbf{L}}_{r-1} = \bar{\mathbf{l}}_{r-1}, L_r^1 = l_r^1, \dots, L_r^{s-1} = l_r^{s-1}) \\ \times f(w_{1,r} Y_r | \bar{\mathbf{A}}_r = \bar{a}_r, \bar{\mathbf{L}}_r = \bar{\mathbf{l}}_r).$$

The equality follows from the knowledge that iterated nested expectation representations of the g-formula can be reexpressed as a traditional g-formula factorization because both representations essentially standardize with respect to the post intervention distribution of the time-dependent confounders [3, 6, 33]. In our case, the outcome is $w_{1,t} Y_t$.

Summarizing the multiple time-point CDRC graphically

Sometimes, we may want to visualize the CDRC graphically, e.g. by plotting $m_t(\bar{a}_t)$ for each t (and stratified by \mathbf{L}_0^* , if meaningful) if the set of strategies is restricted to those that always assign the same value at each time point, see Figure 1c for an illustration. Alternatively, we may opt to plot the CDRC as a function of t , for some selected strategies \bar{a}_t , see Figure 1d. This may be useful if intervention values change over time, or for survival settings.

3.3 Estimation

To estimate the weighted CDRC, we can rely on plug-in estimation of either (13) or (14). That is, we use either a parametric or sequential g-formula type of approach where the (iterated) outcome is multiplied with the respective weight at each time point. As the weighted outcome may possibly have a skewed, complex distribution (depending on the weights), we advocate for the use of (13) as a basis for estimation. This is because estimating the expectation only may then be easier than estimating the whole conditional distribution. In many applications, a data-adaptive estimation approach may be a good choice for modeling the expectation of the weighted outcome. The algorithm in Table 1 presents the detailed steps for a substitution estimator of (13).

For the estimates of the CDRC to be consistent, both the expected weighted (iterated) outcomes and the weights need to be estimated consistently.

Note that for $t = 0$, we suggest to calculate a weighted mean, instead of estimating the weighted expected outcome data-adaptively. This is because the former is typically more stable when Y_0 follows some standard distribution, but w_0 does not. It is a valid strategy as standardizing with respect to the pre-intervention variables L_0 and then calculating the weighted mean of the outcome is identical to standardizing the weighted outcome with respect to L_0 , and then calculating the mean. Another option for $t = 0$ is to facilitate step 6 before step 5 and then create a stacked dataset of the counterfactual outcomes for all intervention values a_0 , and then fit a weighted regression of Y_0 on A_0 , based on the stacked weight vectors. The fitted model can then be used to predict the expected outcome under all a_0 . This strategy is however not explored further in this paper.

3.3.1 Multiple Interventions and Censoring

So far, we have described the case of 1 intervention variable A_t per time point. Of course, it is possible to employ the proposed methodology for multiple intervention variables $\mathbf{A}_t = (A_{t,1}, A_{t,2}, \dots, A_{t,p})$. In this case, one simply has to estimate the conditional densities for all those intervention variables, and taking their product, at each time point. This follows from replacing (10) with $g_s(\mathbf{a}_{s+1} | \mathbf{h}_{s+1})/g_s(\mathbf{a}_{s+1} | \mathbf{a}_s, \mathbf{h}_s)$, and then factorizing the joint intervention distribution based on the assumed time ordering of $(L_s, A_{s,1}, A_{s,2}, \dots, A_{s,p}, Y_s)$. Intervention variables may include censoring variables: we may, for instance, construct CDRC's under the intervention of no censoring. A possible option to apply the proposed methodology is then to recover the estimand $E(Y_t^{\bar{C}_t=0} | A_t = a_t, \dots, A_0 = a_0)$ if there is not enough conditional support for the intervention strategy of interest. Table 1 lists the required modifications of the estimation procedure, based on a time-ordering of $(L_s, A_{s,1}, A_{s,2}, \dots, A_{s,p}, C_s, Y_s)$, $s = 0, \dots, t$. An alternative estimand to recover would be $E(Y_t | C_t = c_t, A_t = a_t, \dots, C_0 = c_0, A_0 = a_0)$. For this, one would require estimating the conditional censoring mechanisms in steps 1a and 1b too. There are however many subtleties and

Table 1: Algorithm for estimating the weighted CDRC at time t

Step 0a:	Define a set of interventions $\bar{\mathcal{A}}_t$, with $ \bar{\mathcal{A}}_t = n_a$ and $\bar{A}_t^{(j)}$ is the j^{th} element of $\bar{\mathcal{A}}_t$, $j = 1, \dots, n_a$.
Step 0b:	Set $\tilde{Y}_t = Y_t$.
For $s = t, \dots, 1$:	
Step 1a:	Estimate the conditional density $g(A_s \mathbf{H}_s)$.
Step 1b:	Estimate the conditional density $g(A_s A_{s-1}, \mathbf{H}_{s-1})$.
Step 2:	Set $a_s = a_s^{(1)}$, where $a_s^{(1)}$ is the s^{th} element of intervention $\bar{A}_t^{(1)} \in \bar{\mathcal{A}}_t$.
Step 3a:	Plug in $a_s^{(1)}$ into the estimated densities from step 1, to calculate $\hat{g}(a_s^{(1)} \mathbf{h}_s)$ and $\hat{g}(a_s^{(1)} a_{s-1}^{(1)}, \mathbf{h}_{s-1})$.
Step 3b:	Calculate the weights $w_s(a_s^{(1)}, c)$ from (12) based on the estimates from 3a. If $\hat{g}(a_s^{(1)} a_{s-1}^{(1)}, \mathbf{h}_{s-1}) \leq c$, estimate $g(a_s^{(1)} a_{s^*}^{(1)}, \mathbf{h}_{s^*})$ as required by the definition of (12) for $s^* = s - 2, \dots, 0$.
Step 4:	Estimate $\mathbb{E}(w_s(a_s^{(1)}, c) \tilde{Y}_s A_s, \mathbf{H}_s)$.
Step 5:	Predict $\tilde{Y}_{s-1} = \hat{\mathbb{E}}(\hat{w}_s(a_s^{(1)}, c) \tilde{Y}_s \bar{A}_s = \bar{a}_s^{(1)}, \mathbf{1}_s)$ based on the fitted model from step 4 and the given intervention $\bar{a}_s^{(1)}$.
For $t = 0$:	
Step 1a:	Estimate the conditional density $g(A_0 \mathbf{L}_0)$.
Step 1b:	Estimate the conditional density $g(A_0)$.
Step 2:	Set $a_0 = a_0^{(1)}$.
Step 3a:	Calculate $\hat{g}(a_0^{(1)} \mathbf{l}_0)$ and $\hat{g}(a_0^{(1)})$.
Step 3b:	Calculate the weights $w_0(a_0^{(1)}, c)$. If $\hat{g}(a_0^{(1)}) \leq c$, then $m_{w,t}(\bar{a}_t^{(1)}, c)$ is undefined.
Step 4:	Estimate $\mathbb{E}(w_0(a_0^{(1)}, c) \tilde{Y}_0 A_0, \mathbf{L}_0)$.
Step 5:	Calculate $\hat{m}_{w,t}(\bar{a}_t^{(1)}, c) = \hat{\mathbb{E}}_{w(c)}(Y_t^{\bar{a}_t^{(1)}}) = (\sum_i w_{0,i})^{-1} (\hat{w}_0(a_0^{(1)}, c)^T \tilde{Y}_0)$; that is, obtain the estimate of the weighted CDRC at $\bar{a}_t^{(1)}$ through calculating the weighted mean.
Then:	
Step 6:	Repeat steps 2-5 for the other interventions $\bar{A}_t^{(j)}$, $j = 2, \dots, n_a$. This yields an estimate of the desired dose-response curve (5) at t .

Time-to-event data:

Possible changes, to recover $E(Y_t^{\bar{C}_t=0} | A_t = a_t, \dots, A_0 = a_0)$ if there is not enough support for $\bar{A}_t^{(j)}$.

Step 1a/b: Estimate the densities among those uncensored, and without prior event ($C_t = 0, Y_{t-1} = 0$).

Step 2: Also, set $c_t = 0$ (we only describe the setting where we intervene on censoring).

Step 4: Fit the model for the weighted outcome among those uncensored and without prior event, that is, estimate $\mathbb{E}(w_t(a_t^{(1)}, c) \tilde{Y}_t | \bar{A}_t, C_t = 0, Y_{t-1} = 0, \mathbf{H}_t)$.

Step 5: Additionally, set $\tilde{Y}_{t-1,i} = 1$, if $Y_{t-2,i} = 1$.

dangers related to the interpretation and estimation of CDRC's under censoring, and possibly competing events; for example, conditioning on the censoring indicators may lead to collider bias, intervening the on censoring mechanisms to direct effect estimands [34], identification assumptions need to be refined and generic time-orderings where treatment variables are separated by different blocks of confounders may lead to more iterated expectations that have to be fitted. Those details go beyond the scope of this paper.

3.3.2 On Practical Violations of the Positivity Assumption and Diagnostics

The positivity assumption, as defined in (7), is a strong requirement. It is however important to highlight that in many practical applications one may not be interested in all possible intervention histories, but only in a (very restricted) subset of intervention trajectories – and thus only in some parts of the full CDRC. For instance, in the data example, we are only interested in positive drug concentrations (<10 mg/L) and in intervention strategies where the concentration is constant over time; complex concentration trajectories, where values increase and decrease, and more generally fluctuate over time do not relate to the most meaningful scientific estimands in this case. It is therefore likely that we require the positivity assumption to only hold for particular areas of the conditional treatment densities; and that we can evaluate those

areas as a diagnostic tool. Let $\bar{\mathcal{A}}_t$ be the set of interventions of interest, with $|\bar{\mathcal{A}}_t| = n_a \ll \infty$ and $\bar{\mathcal{A}}_t^{(j)} = (a_0^{(j)}, \dots, a_t^{(j)})$ is the j^{th} element of $\bar{\mathcal{A}}_t$, $j = 1, \dots, n_a$. Suppose the intervention values at t are already ordered such that $a_t^{(1)} < a_t^{(2)} < \dots < a_t^{(n_a)}$. Then we can *approximate* the relevant parts of conditional treatment densities with a *binning strategy* in the sense that we calculate

$$P \left(a_t^{(j)} \in \left[a_t^{(j)} - \frac{1}{2}(a_t^{(j)} - a_t^{(j-1)}); a_t^{(j)} + \frac{1}{2}(a_t^{(j)} - a_t^{(j+1)}) \right) \middle| \bar{a}_{t-1}^{(j)} \in \left[a_{t-1}^{(j)} - \frac{1}{2}(a_{t-1}^{(j)} - a_{t-1}^{(j-1)}); a_{t-1}^{(j)} + \frac{1}{2}(a_{t-1}^{(j)} - a_{t-1}^{(j+1)}) \right], \bar{l}_t \right); \quad (15)$$

that is, we want to estimate the probability to approximately observe the intervention value $a_t^{(j)}$ under strategy j , given that one has followed the same strategy of interest j so far (until $t-1$), and irrespective of the covariate history. Alternatively, instead of defining the bin widths through the intervention values of interest, we may calculate them data-adaptively [35]. Estimating the mean of those probabilities over all observed \bar{l}_t in a particular data set serves as diagnostic tool to measure the support for each rule j , at each time point. Note that we can relax the positivity assumption further for standard g-computation analyses, if we are willing to assume that the parametric modeling assumptions at the estimation stage are complex enough to extrapolate into regions of low support [36]. We propose to estimate (15) with standard regression techniques, and present a summary of those probabilities as a rough measure of support for each intervention trajectory of interest. With this, one may judge where standard g-computation estimates are more reliable, and where they may be best complemented with weighted CDRCs using the projection functions presented above.

4 Monte-Carlo Simulations

In this section, we evaluate the proposed methods in three different simulation settings. Simulation 1 considers a very simple setting, as a basic reference for all approaches presented. In simulation 2, a survival setting is considered, to explore the stability of standard, unweighted g-computation in more sophisticated setups. The third simulation is complex, and inspired by the data-generating process of the data analysis. It serves as the most realistic setup for all method evaluations.

Data Generating Processes & Estimands

Simulation 1: We simulated both a binary and normally distributed confounder, a continuous (normally distributed) intervention and a normally distributed outcome – for 3 time points and a sample size of $n = 10,000$. The exact model specifications are given in Appendix B.1. The intervention strategies of interest comprised intervention values in the interval $[2, 11]$ which were constant over time; that is, $\bar{\mathcal{A}}_t^1 = \{(2, 2, 2), \dots, (11, 11, 11)\}$. The primary estimand ψ^1 is the CDRC (5) for $t = 1, 2, 3$, $\mathbf{L}_0^* = \emptyset$ and all $\bar{a}_t \in \bar{\mathcal{A}}_t^1$. The secondary estimand ψ_w^1 is the weighted CDRC defined through (9), with the weights (12), for the same intervention strategies.

Simulation 2: We simulated a continuous (normally distributed) intervention, two covariates (one of which is a confounder), an event outcome and a censoring indicator – for 5 time points and varying sample sizes of $n_1 = 500, n_2 = 1,000, n_3 = 10,000$ and $n_4 = 50,000$. The exact model specifications are given in Appendix B.2. The intervention strategies of interest comprised intervention values in the interval $[-7, 13]$ which were constant over time; that is, $\bar{\mathcal{A}}_t^2 = \{(-7, -7, -7, -7, -7), \dots, (13, 13, 13, 13, 13)\}$. The estimand ψ^2 is the CDRC (5) for $t = 1, 2, 3, 4, 5$, $\mathbf{L}_0^* = \emptyset$, all $\bar{a}_t \in \bar{\mathcal{A}}_t^2$ and under no censoring ($\bar{c}_t = (0, \dots, 0)$).

Simulation 3: We simulated data inspired by the data generating process of the data example outlined in Sections 2 and 5 as well as Figure 3. The continuous intervention refers to drug concentration (of evavirenz), modeled through a truncated normal distribution. The binary outcome of interest is viral failure. Time-varying confounders, affected by prior interventions, are weight and adherence. Other variables include co-morbidities and drug dose (time-varying) as well as sex, genotype, age and NRTI regimen.

We considered 5 clinic visits and a sample size of $n = 1.000$. The exact model specifications are given in Appendix B.3. The intervention strategies of interest comprised concentration values in the interval $[0, 10]$ which were constant over time; that is, $\bar{\mathcal{A}}_t^3 = \{(0, 0, 0, 0, 0), \dots, (10, 10, 10, 10, 10)\}$. The primary estimand ψ_3 is the CDRC (5) for $t = 1, 2, 3, 4, 5$, $\mathbf{L}_0^* = \emptyset$ and all $\bar{a}_t \in \bar{\mathcal{A}}_t^3$. The secondary estimand ψ_w^3 is the weighted CDRC (9) with the weights (12) for the same intervention strategies.

Estimation & Evaluation

All simulations were evaluated based on the results of $\mathcal{R} = 1.000$ simulation runs. We evaluated the bias of estimating ψ^1, ψ^2 and ψ^3 with standard parametric g -computation with respect to the true CDRC. In simulations 1 and 3 model specification for g -computation was based on variable screening with LASSO, simulation 2 explored the idealized setting of using correct model specifications. We further evaluated the bias of the estimated weighted CDRC with the true weighted CDRC, for $c = 1$; i.e. we looked whether $E(Y_t|A_t = a_t, \dots, A_0 = a_0)$ could be recovered for every intervention strategy of interest. Estimation was based on the algorithm of Table 1. The density estimates, which are required for estimating the weights, were based on both appropriate parametric regression models (that is, linear regression) and binning the continuous intervention into intervals; a computationally more sophisticated data-adaptive approach for density estimation is considered in Section 5. We then compared the estimated CDRC and weighted CDRC ($c = 1$) with other weighted CDRC's where $c = 0.01$ and $c = 0.001$. To estimate the iterated conditional expectations of the weighted outcome, we used super learning, i.e. a data adaptive approach [4]. Our learner sets included different generalized linear (additive) regression models (with penalized splines, and optionally interactions), multivariate adaptive regression splines, LASSO estimates and regression trees – after prior variable screening with LASSO and Cramer's V [37]. Lastly, we visualize the conditional support of all considered intervention strategies, in all simulations, as suggested in (15).

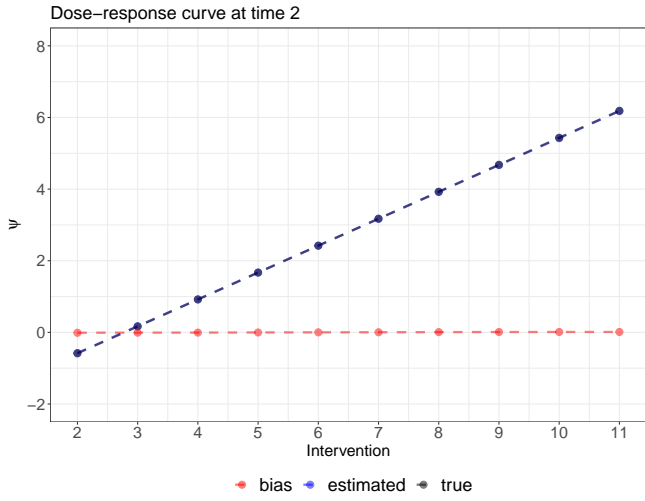
Results

The results of the simulations are summarized in Figures 2, 5 and 6.

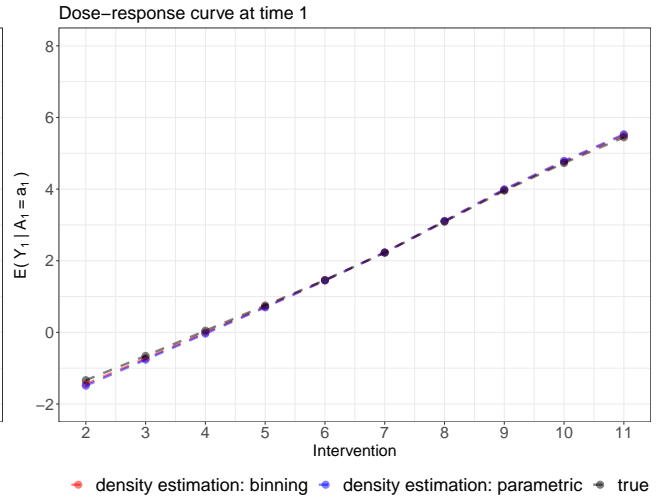
In simulation 1, applying standard g -computation to the continuous intervention led to approximately unbiased estimates for all intervention values, through all time points (Figure 2a); and independent of the level of support (Figure 6a). The weighted CDRC, with $c = 1$, recovered the association $E(Y_1|A_1 = a_1)$ perfectly for the first time point, independent of the density estimation strategy (Figure 2b). For later time points, some bias can be observed in regions of lower support (i.e., for intervention values between 9 and 11), see Figure 5a.

Simulation 2 shows a setting in which g -computation estimates for the CDRC are not always unbiased, despite correct model specifications! Figure 2c visualizes this finding for the fifth time point: it can be seen that a sample size of ≥ 10.000 is needed for approximately unbiased estimation of the CDRC over the range of all intervention strategies. Note, however, that for some time points lower sample sizes are sufficient to guarantee unbiased estimation (Figure 5b).

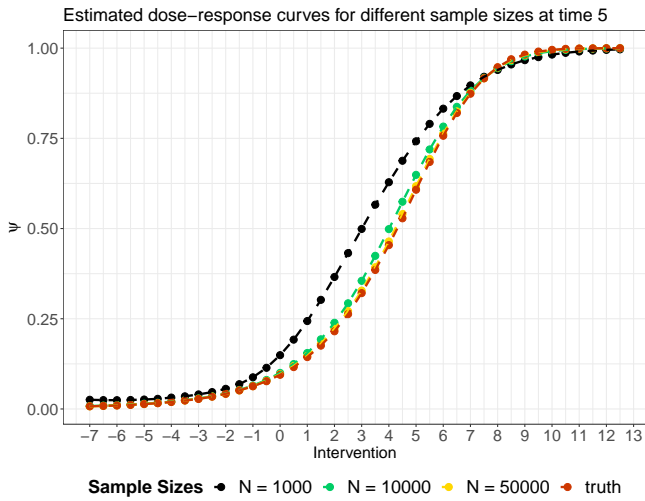
The most sophisticated simulation setting 3 reveals some more features of the proposed methods. First, we can see that in areas of lowest support, towards concentration values close to zero, there is relevant bias of a standard g -computation analysis (Figure 2d); whereas in areas of reasonable to good support the CDRC estimates are approximately unbiased. The weighted CDRC with $c = 1$ can recover the associations $E(Y_t|A_t = a_t, \dots, A_1 = a_1)$ for intervention values ≥ 1 , but there is some bias as the most critical area close to zero is approached, independent of the method used for estimating the weights (Figure 2e, and also Figure 5d). Both Figure 2f and Figure 5e highlight the behaviour of the weighted CDRC for $c = 0.01$ and $c = 0.001$: it can be clearly seen that the curves represent a compromise between the CDRC and the association represented by the weighted CDRC (with $c = 1$). Evaluating the results for intervention values of zero, shows that weighting the curve in areas of low support yields to a compromise that moves the CDRC away from the estimated high probabilities of viral failure to more moderate values informed by the observed association. Knowledge of this behaviour may be informative for the data analysis below.



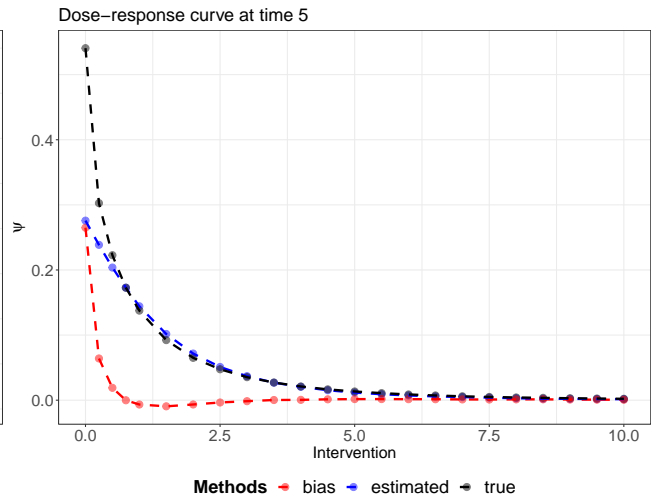
(a) Simulation 1: true and estimated CDRC at $t = 2$



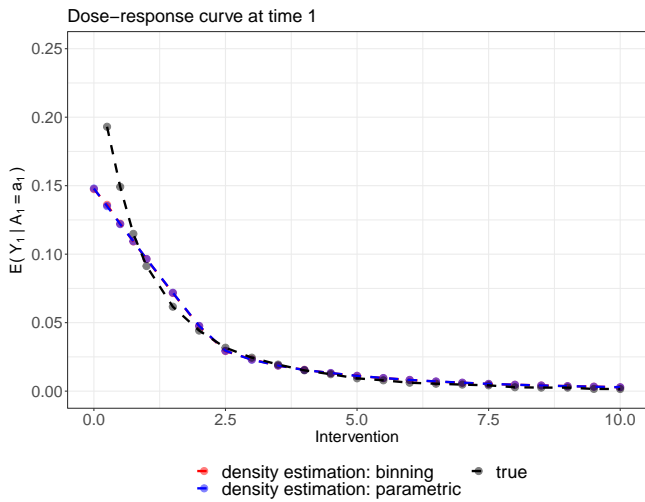
(b) Simulation 1: weighted CDRC, $c = 1, t = 1$



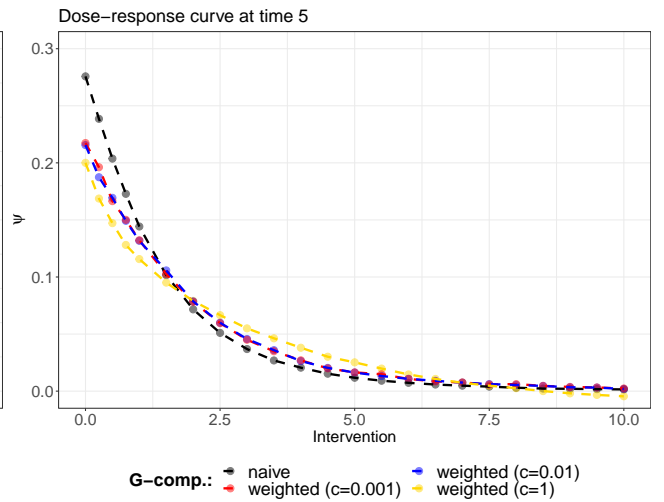
(c) Simulation 2: true and estimated CDRC at $t = 5$



(d) Simulation 3: true and estimated CDRC at $t = 5$



(e) Simulation 3: weighted CDRC, $c = 1, t = 1$



(f) Simulation 3: CDRC's, $t = 5, c = 0.001, 0.01, 1$

Figure 2: Results of the Monte-Carlo simulations

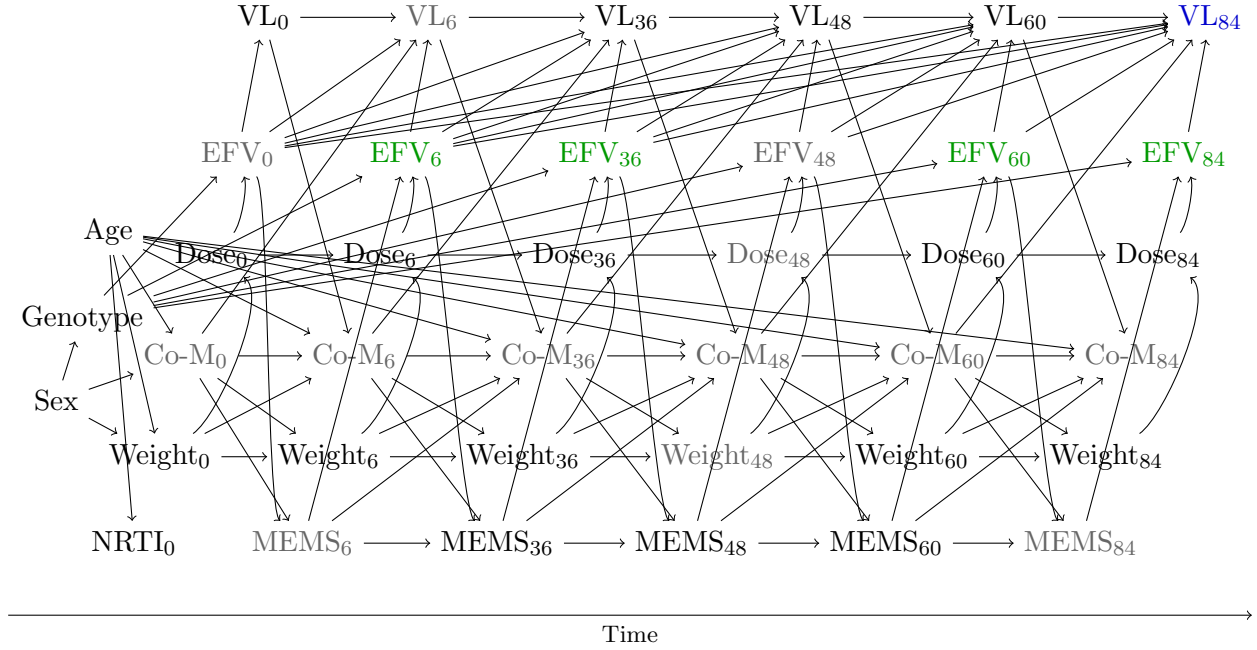


Figure 3: Directed Acyclic graph for the data analysis. The intervention variable is shown in green (efavirenz concentration), the outcome in blue (viral load at the end of follow-up). Unmeasured variables are colored in grey. Both MEMS and weight are time-dependent confounders which are affected by prior treatment nodes.

5 Data Analysis

We now illustrate the ideas based on the data from Bienczak et al. [25], introduced in Section 2. We consider the trial visits at $t = 0, 6, 36, 48, 60, 84$ weeks of 125 children on an efavirenz-based treatment regime. The intervention of interest is efavirenz mid-dose interval concentration (A_t), defined as plasma concentration (in mg/L) 12 hours after dose; the outcome is viral failure (Y_t , defined as > 100 copies/mL). Measured baseline variables, which we included in the analysis, are $\mathbf{L}_0 = \{\text{sex, genotype, age, the nucleoside reverse transcriptase inhibitors drug (NRTI), weight}\}$. Genotype refers to the metabolism status (slow, intermediate, extensive) related to the single nucleotide polymorphisms in the CYP2B6 gene, which is relevant for metabolizing efavirenz and directly affects its concentration in the body. Measured follow-up variables are $\mathbf{L}_t = \{\text{weight, adherence (measured through memory caps, MEMS), dose}\}$.

The assumed data generating process is visualized in the DAG in Figure 3, and explained in more detail in Appendix C. Briefly, both weight and adherence are time-dependent confounders, potentially affected by prior concentration trajectories, which are needed for identification of the CDRC.

Our target estimands are the CDRC (5) and the weighted CDRC (9) at $t = 84$ weeks. The intervention strategies of interest are $\bar{A}_t = \{(0, 0, 0, 0), \dots, (10, 10, 10, 10)\}$.

The analysis illustrates the ideas based on a complete case analysis of all measured variables represented in the DAG ($n = 58$), but excluding dose (not needed for identification) and MEMS (due to the high proportion of missingness).

We estimated the CDRC both with sequential and parametric g-computation using the intervention strategies \bar{A}_t . The estimation of the weighted CDRC followed the algorithm of Table 1. The conditional treatment densities, which are needed for the construction of the weights, were estimated both parametrically based on the implied distributions from linear models (for concentrations under $5 mg/L$) and with highly-adaptive LASSO conditional density estimation (for concentrations $\geq 5 mg/L$) [38, 39]. This is because the density in the lower concentration regions were approximately normally distributed, but more complex for higher values.

The conditional expectation of the weighted outcome (Step 4 of the algorithm) was estimated data-adaptively with super learning using the following learning algorithms: the highly adaptive LASSO,

multivariate adaptive regression splines, generalized linear models (also with interactions), generalized additive models as well as the mean and median. Prior variable screening, which was essential given the small sample size, was based on both the LASSO and Cramer’s V .

We estimated the weighted CDRC for $c = 0.001, 0.01, 1$. We also calculate the support of the continuous intervention strategies $\bar{\mathcal{A}}_t$ through estimating (15).

Results

The main results of the analyses are given in Figure 4.

Figures 4a and 4b show that the estimated CDRC (black solid line) suggests higher probabilities of failure with lower concentration values. The curve is steep in the region from 0 – 2mg, which is even more pronounced for parametric g-computation when compared to sequential g-computation (Figure 5f).

Both Figures 4a and 6d illustrate the low level of (conditional support) support for extremely small concentration values close to 0 mg/L and for very large concentrations. Note that in Figure 4a the area shaded in dark blue relates to an estimated conditional support, averaged over all time points, of 0, the light blue areas to support levels greater 0, but smaller 0.01 and the white areas to all other support levels.

The weighted curves, shown in Figure 4b, highlight how in these areas of low support the curves differ markedly. The weighted curves are less steep in the crucial areas close to zero and –as in the simulation studies– we observe a tendency of the curves with $c = 0.01$ and $c = 0.001$ to provide a visual compromise between the CDRC and the estimand recovering the relevant association ($c = 1$). The weighted curves show the probability of failure if patients whose covariate trajectory make the concentration (trajectory) of interest not completely unlikely to occur actually “get” the concentration of interest, and all other patients would have concentration trajectories such that their outcomes are comparable to the patient population with the respective concentration trajectory of interest. For example, if we are interested in the counterfactual failure probability under a concentration of 10 mg/L, but the covariate trajectory makes this value seem highly unlikely for a patient (e.g., because they are fast metabolizers and would not be able to achieve this level), then this patient would be evaluated under different concentrations which produce outcomes as we would typically see in patients with 10 mg/L.

The practical implication is that if we don’t want to rely on parametric extrapolation in regions of low support, and then also make use of the observed marginal associations through our projection function, we should be careful in assigning too much meaning to the actual estimated failure values at around 0 (and > 6) mg/L, e.g. we may not argue with the steepness of the CDRC close to 0 when proposing particular lower limits of target concentrations; possibly also because we may not regard very low/high concentrations trajectories likely to be achievable for a subset of patients.

In Figure 4c kernel density estimates of the weights are displayed, both for the follow-up visits at 6 and 84 weeks and for $A = 1$ and $A = 0$ mg/L. All estimated weight distributions are stable in the sense that no “extreme” estimated weights are present; this may be interpreted as reassuring in terms of the chosen estimation strategy. The smaller c , the more centered are the weights around 1: this is because the weights are only different from 1 if the conditional support level is below c . This is obviously always the case for $c = 1$, where the weight distribution is rather skewed.

6 Discussion

We have introduced and evaluated various methods for causal effect estimation with continuous multiple time-point interventions. As an obvious first step, we investigated standard (parametric or sequential) g-formula based approaches for identification and estimation of the actual causal dose-response curve. We emphasized that this has the advantage of sticking to the estimand of interest, but with a relatively strong positivity assumption which will likely be violated in most data analyses. Our simulations were designed to explore how well such a standard approach may extrapolate in sparse data regions and how the approach performs in both simple and complex settings. We found that in simple scenarios the CDRC estimates were approximately unbiased, but that in more complex settings sometimes large sample sizes were needed for good performance and that in regions of very poor support a relatively large bias could be

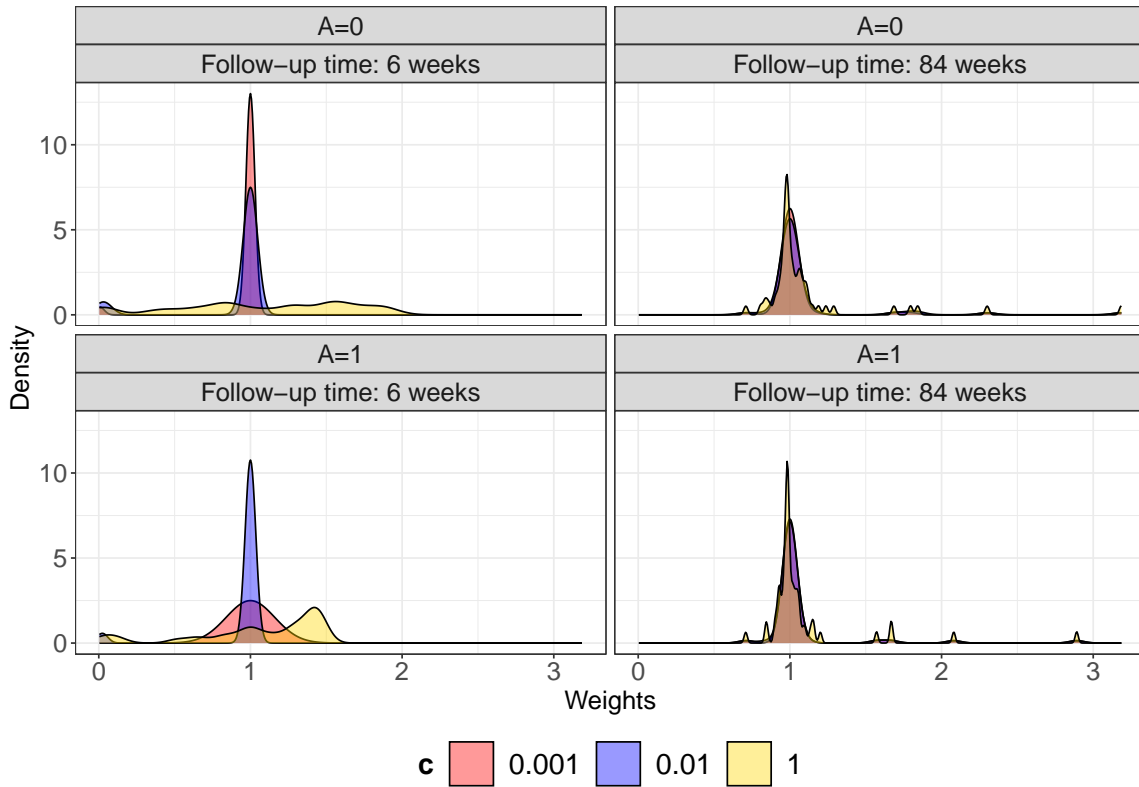
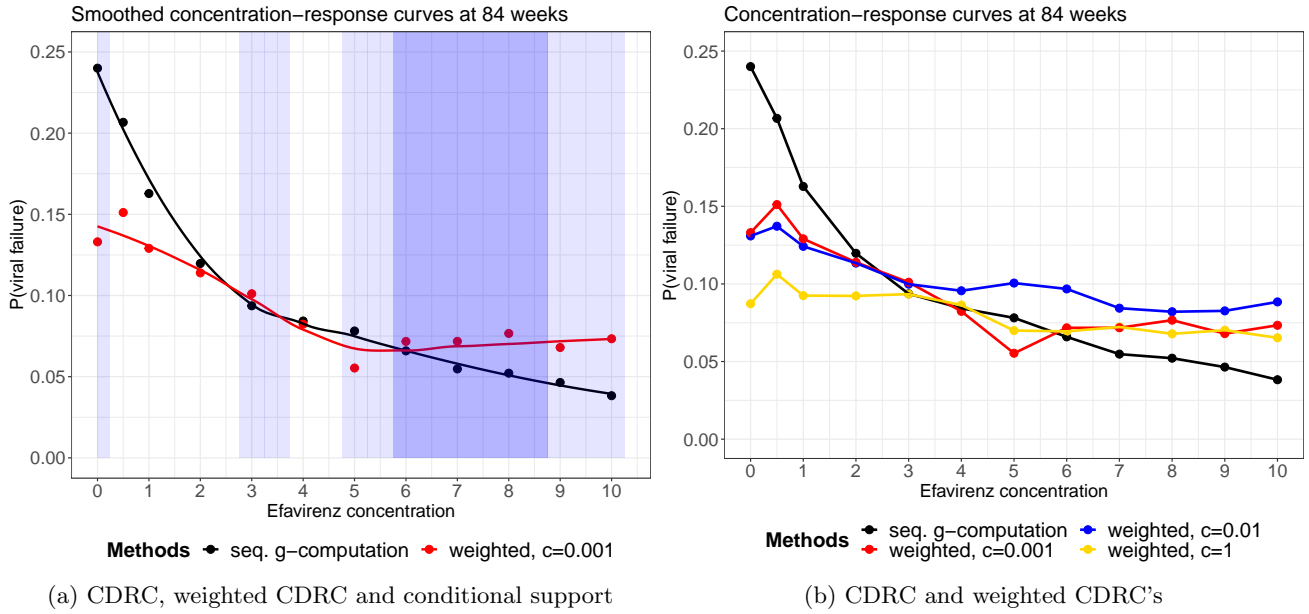


Figure 4: Results of the data analysis

observed. These findings suggest that the toolkit for causal effect estimation with longitudinal continuous interventions should therefore ideally be broader.

A first pragmatic approach to tackle positivity violations is to weigh those estimates of the CDRC down, which are related to interventions that have little or no support in the data. This has already been proposed in the point treatment case for estimands that are defined through parameters in a marginal structural working model (MSM) [36]; or, more generally for MSM parameters which summarize features of longitudinal *binary* interventions [31]. Suggested choices for the weight function include the marginal

support for each intervention. We discussed that this choice, as well similar choices based on the same rationale, entail a compromise between the CDRC and a weighted CDRC in areas of low support, but lack an intuitive interpretation and do not relate to a clear estimand. We have therefore advocated to rather use weights that recover the CDRC if there is enough support, and a meaningful estimand which doesn't require the positivity assumption otherwise.

Based on this rationale we proposed a weight function which returns the CDRC under enough conditional support, and the crude association between the outcome at time t and the treatment history otherwise. This choice ensures that the estimand is always well-defined and provides a natural compromise between causation and association in areas of low support. Our simulations suggest that the provided estimation algorithm for the weighted CDRC can indeed successfully recover the associational estimand and illustrate the compromise that is practically achieved. As the proposed weights may have skewed distributions, we highlighted the importance of using a data-adaptive estimation approach.

We hope that our manuscript has shown that for continuous multiple time point interventions one has to ultimately make a tradeoff between estimating the CDRC as closely as possible, at the risk of bias due to positivity violations and minimizing the risk of bias due to positivity violations, at the cost of redefining the estimand. If the scientific question of interest allows a redefinition of the estimand in terms of longitudinal modified treatment policies [23] then this may be a great choice. Otherwise, it may be helpful to use g-computation algorithms for continuous interventions, visualize the estimates in appropriate curves, calculate the diagnostics (15) by estimating the conditional support and then estimate the proposed weighted CDRCs as a magnifying glass for the curve's behaviour in areas of low support.

Our suggestions can be extended in several directions: it may be possible to design different weight functions that keep the spirit of modifying estimands under continuous interventions only in areas of low support; the extent of the compromise, controlled by the tuning parameter c , may be chosen data-adaptively and our basic considerations for time-to-event data may be extended to cover more estimands, particular in the presence of competing risks.

Acknowledgements

We are grateful for the support of the CHAPAS-3 trial team, their advise regarding the illustrative data analysis and making their data available to us. We would like to particularly thank David Burger, Sarah Walker, Di Gibb, Andrzej Bieniczak and Elizabeth Kaudha. We would also like to acknowledge Daniel Saggau, who has contributed to the data-generating processes of our simulation setups and Igor Stojkov for contributing substantive knowledge to pharmacological angles relevant to the data example. Computations were performed using facilities provided by the University of Cape Town's ICTS High Performance Computing team. Michael Schomaker is supported by the German Research Foundations (DFG) Heisenberg Programm (grants 465412241 and 465412441).

References

- [1] J. M. Robins, M. A. Hernan, and B. Brumback. Marginal structural models and causal inference in epidemiology. *Epidemiology*, 11(5):550–560, 2000.
- [2] J. Robins. A new approach to causal inference in mortality studies with a sustained exposure period - application to control of the healthy worker survivor effect. *Mathematical Modelling*, 7(9-12):1393–1512, 1986.
- [3] H. Bang and J. M. Robins. Doubly robust estimation in missing data and causal inference models. *Biometrics*, 64(2): 962–972, 2005.
- [4] M. Van der Laan and S. Rose. *Targeted Learning*. Springer, 2011.
- [5] M. E. Schnitzer, M. J. van der Laan, E. E. Moodie, and R. W. Platt. Effect of breastfeeding on gastrointestinal infection in infants: A targeted maximum likelihood approach for clustered longitudinal data. *Annals of Applied Statistics*, 8(2): 703–725, 2014.
- [6] M. Schomaker, M. A. Luque Fernandez, V. Leroy, and M. A. Davies. Using longitudinal targeted maximum likelihood estimation in complex settings with dynamic interventions. *Statistics in Medicine*, 38:4888–4911, 2019.

- [7] P. Baumann, M. Schomaker, and E. Rossi. Estimating the effect of central bank independence on inflation using longitudinal targeted maximum likelihood estimation. *Journal of Causal Inference*, 9(1):109–146, 2021.
- [8] H. Bell-Gorrod, M.P. Fox, A. Boulle, H. Prozesky, R. Wood, F. Tanser, M.A. Davies, and M. Schomaker. The impact of delayed switch to second-line antiretroviral therapy on mortality, depending on failure time definition and CD4 count at failure. *American Journal of Epidemiology*, 189:811–819, 2020.
- [9] L. E. Cain, M. S. Saag, M. Petersen, M. T. May, S. M. Ingle, R. Logan, J. M. Robins, S. Abgrall, B. E. Shepherd, S. G. Deeks, M. John Gill, G. Touloumi, G. Vourli, F. Dabis, M. A. Vandenhende, P. Reiss, A. van Sighem, H. Samji, R. S. Hogg, J. Rybniker, C. A. Sabin, S. Jose, J. Del Amo, S. Moreno, B. Rodriguez, A. Cozzi-Lepri, S. L. Boswell, C. Stephan, S. Perez-Hoyos, I. Jarrin, J. L. Guest, A. D’Arminio Monforte, A. Antinori, R. Moore, C. N. Campbell, J. Casabona, L. Meyer, R. Seng, A. N. Phillips, H. C. Bucher, M. Egger, M. J. Mugavero, R. Haubrich, E. H. Geng, A. Olson, J. J. Eron, S. Napravnik, M. M. Kitahata, S. E. Van Rompaey, R. Teira, A. C. Justice, J. P. Tate, D. Costagliola, J. A. Sterne, and M. A. Hernan. Using observational data to emulate a randomized trial of dynamic treatment-switching strategies: an application to antiretroviral therapy. *International Journal of Epidemiology*, 45(6):2038–2049, 2016.
- [10] Noémi Kreif, Linh Tran, Richard Grieve, Bianca De Stavola, Robert C Tasker, and Maya Petersen. Estimating the Comparative Effectiveness of Feeding Interventions in the Pediatric Intensive Care Unit: A Demonstration of Longitudinal Targeted Maximum Likelihood Estimation. *American Journal of Epidemiology*, 186(12):1370–1379, 2017.
- [11] Keisuke Hirano and Guido W. Imbens. *The Propensity Score with Continuous Treatments*, chapter 7, pages 73–84. Wiley, 2004.
- [12] Noémi Kreif, Richard Grieve, Iván Díaz, and David Harrison. Evaluation of the effect of a continuous treatment: A machine learning approach with an application to treatment for traumatic brain injury. *Health Economics*, 24(9):1213–1228, 2015.
- [13] Edward H. Kennedy, Zongming Ma, Matthew McHugh, and Dylan S. Small. Nonparametric methods for doubly robust estimation of continuous treatment effects. *Journal of the Royal Statistical Society. Series B, Statistical methodology*, 79:1229–1245, 2017.
- [14] Ted Westling, Peter Gilbert, and Marco Carone. Causal isotonic regression. *Journal of the Royal Statistical Society, Series B*, 82:719–747, 2020.
- [15] Zhiwei Zhang, Jie Zhou, Weihua Cao, and Jun Zhang. Causal inference with a quantitative exposure. *Statistical Methods in Medical Research*, 25(1):315–335, 2016.
- [16] Antonio F. Galvao and Liang Wang. Uniformly semiparametric efficient estimation of treatment effects with a continuous treatment. *Journal of the American Statistical Association*, 110(512):1528–1542, 2015.
- [17] Tyler J. VanderWeele, Yu Chen, and Habibur Ahsan. Inference for causal interactions for continuous exposures under dichotomization. *Biometrics*, 67(4):1414–1421, 2011.
- [18] Iván Díaz and Mark J. van der Laan. Targeted data adaptive estimation of the causal dose–response curve. *Journal of Causal Inference*, 1(2):171–192, 2013.
- [19] R. Neugebauer and M. van der Laan. Nonparametric causal effects based on marginal structural models. *Journal of Statistical Planning and Inference*, 137(2):419–434, 2007.
- [20] S. Goetgeluk, S. Vansteelandt, and E. Goetghebeur. Estimation of controlled direct effects. *Journal of the Royal Statistical Society Series B-Statistical Methodology*, 70:1049–1066, 2008.
- [21] Jessica G. Young, Miguel A. Hernan, and James M. Robins. Identification, estimation and approximation of risk under interventions that depend on the natural value of treatment using observational data. *Epidemiologic Methods*, 3(1):1–19, 2014.
- [22] Jessica G. Young, Roger W. Logan, James M. Robins, and Miguel A. Hernán. Inverse probability weighted estimation of risk under representative interventions in observational studies. *Journal of the American Statistical Association*, 114(526):938–947, 2019.
- [23] Iván Díaz, Nicholas Williams, Katherine L. Hoffman, and Edward J. Schenck. Non-parametric causal effects based on longitudinal modified treatment policies. *Journal of the American Statistical Association*, in press, 2021.
- [24] Veronica Mulenga, Victor Musiime, Adeodata Kekitiinwa, Adrian D. Cook, George Abongomera, Julia Kenny, Chisala Chabala, Grace Mirembe, Alice Asimwe, Ellen Owen-Powell, David Burger, Helen McIlleron, Nigel Klein, Chifumbe Chintu, Margaret J. Thomason, Cissy Kityo, A. Sarah Walker, and Diana Gibb. Abacavir, zidovudine, or stavudine as paediatric tablets for african hiv-infected children (chapas-3): an open-label, parallel-group, randomised controlled trial. *The Lancet Infectious Diseases*, 16(2):169–79, 2016.

- [25] Andrzej Bienczak, Paolo Denti, Adrian Cook, Lubbe Wiesner, Veronica Mulenga, Cissy Kityo, Addy Kekitiinwa, Diana M. Gibb, David Burger, A. Sarah Walker, and Helen McIlleron. Plasma efavirenz exposure, sex, and age predict virological response in hiv-infected african children. *Journal of Acquired Immune Deficiency Syndromes*, 73(2):161–168, 2016.
- [26] Andrzej Bienczak, Paolo Denti, Adrian Cook, Lubbe Wiesner, Veronica Mulenga, Cissy Kityo, Addy Kekitiinwa, Diana M. Gibb, David Burger, Ann S. Walker, and Helen McIlleron. Determinants of virological outcome and adverse events in african children treated with paediatric nevirapine fixed-dose-combination tablets. *AIDS*, 31(7):905–915, 2017.
- [27] R. R. Moholisa, M. Schomaker, L. Kuhn, S. Meredith, L. Wiesner, A. Coovadia, R. Strehlau, L. Martens, E. J. Abrams, G. Maartens, and H. McIlleron. Plasma lopinavir concentrations predict virological failure in a cohort of South African children initiating a protease-inhibitor-based regimen. *Antiviral Therapy*, 19(4), 2014.
- [28] R. R. Moholisa, M. Schomaker, L. Kuhn, S. Castel, L. Wiesner, A. Coovadia, R. Strehlau, F. Patel, F. Pinillos, E. J. Abrams, G. Maartens, and H. McIlleron. Effect of lopinavir and nevirapine concentrations on viral outcomes in protease inhibitor-experienced HIV-infected children. *Pediatric Infectious Disease Journal*, 35(12):e378–e383, 2016.
- [29] Catherine Orrell, Andrzej Bienczak, Karen Cohen, David Bangsberg, Robin Wood, Gary Maartens, and Paolo Denti. Effect of mid-dose efavirenz concentrations and CYP2B6 genotype on viral suppression in patients on first-line antiretroviral therapy. *International Journal of Antimicrobial Agents*, 47(6):466–472, 2016.
- [30] M. Hernan and J. Robins. *Causal inference*. Chapman & Hall/CRC, Boca Raton, 2020. URL <https://www.hsph.harvard.edu/miguel-hernan/causal-inference-book/>.
- [31] M. Petersen, J. Schwab, S. Gruber, N. Blaser, M. Schomaker, and M. van der Laan. Targeted maximum likelihood estimation for dynamic and static longitudinal marginal structural working models. *Journal of Causal Inference*, 2(2):147–185, 2014.
- [32] M. J. van der Laan and S. Gruber. Targeted minimum loss based estimation of causal effects of multiple time point interventions. *International Journal of Biostatistics*, 8(1):article 9, 2012.
- [33] M. L. Petersen. Commentary: Applying a causal road map in settings with time-dependent confounding. *Epidemiology*, 25(6):898–901, 2014.
- [34] J. G. Young, M. J. Stensrud, E. J. T. Tchetgen, and M. A. Hernan. A causal framework for classical statistical estimands in failure-time settings with competing events. *Statistics in Medicine*, 39(8):1199–1236, 2020.
- [35] Iván Díaz and Mark van der Laan. Super learner based conditional density estimation with application to marginal structural models. *The International Journal of Biostatistics*, 7(1):Article 38, 2011. URL <https://doi.org/10.2202/1557-4679.1356>.
- [36] M. L. Petersen, K. E. Porter, S. Gruber, Y. Wang, and M. J. van der Laan. Diagnosing and responding to violations in the positivity assumption. *Statistical Methods in Medical Research*, 21(1):31–54, 2012.
- [37] C. Heumann, M. Schomaker, and Shalabh. *Introduction to Statistics and Data Analysis - With Exercises, Solutions and Applications in R*. Springer, Heidelberg, 2023.
- [38] Nima S Hejazi, David Benkeser, and Mark J van der Laan. *haldensify: Highly adaptive lasso conditional density estimation*, 2022. URL <https://github.com/nhejazi/haldensify>. R package version 0.2.3.
- [39] Nima S. Hejazi, Mark J. van der Laan, and David Benkeser. ‘haldensify’: Highly adaptive lasso conditional density estimation in ‘r’. *Journal of Open Source Software*, 7(77):4522, 2022. doi: 10.21105/joss.04522. URL <https://doi.org/10.21105/joss.04522>.
- [40] A. Bienczak, A. Cook, L. Wiesner, A. Olagunju, V. Mulenga, C. Kityo, A. Kekitiinwa, A. Owen, A. S. Walker, D. M. Gibb, H. McIlleron, D. Burger, and P. Denti. The impact of genetic polymorphisms on the pharmacokinetics of efavirenz in african children. *British Journal of Clinical Pharmacology*, 82(1):185–98, 2016.

A Additional Results

A.1 Simulation and Analysis Results

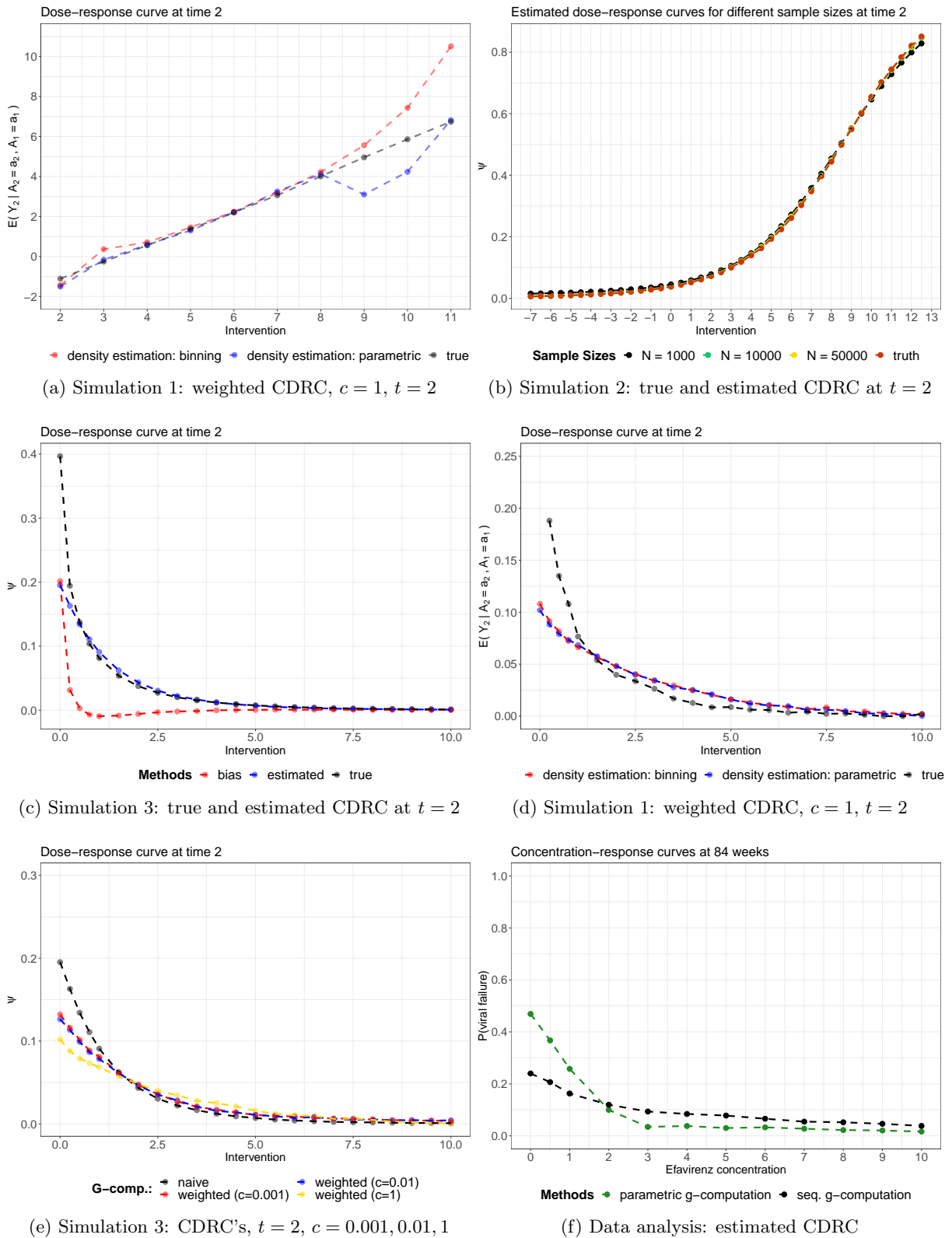


Figure 5: Additional simulation and analysis results

A.2 Intervention Support

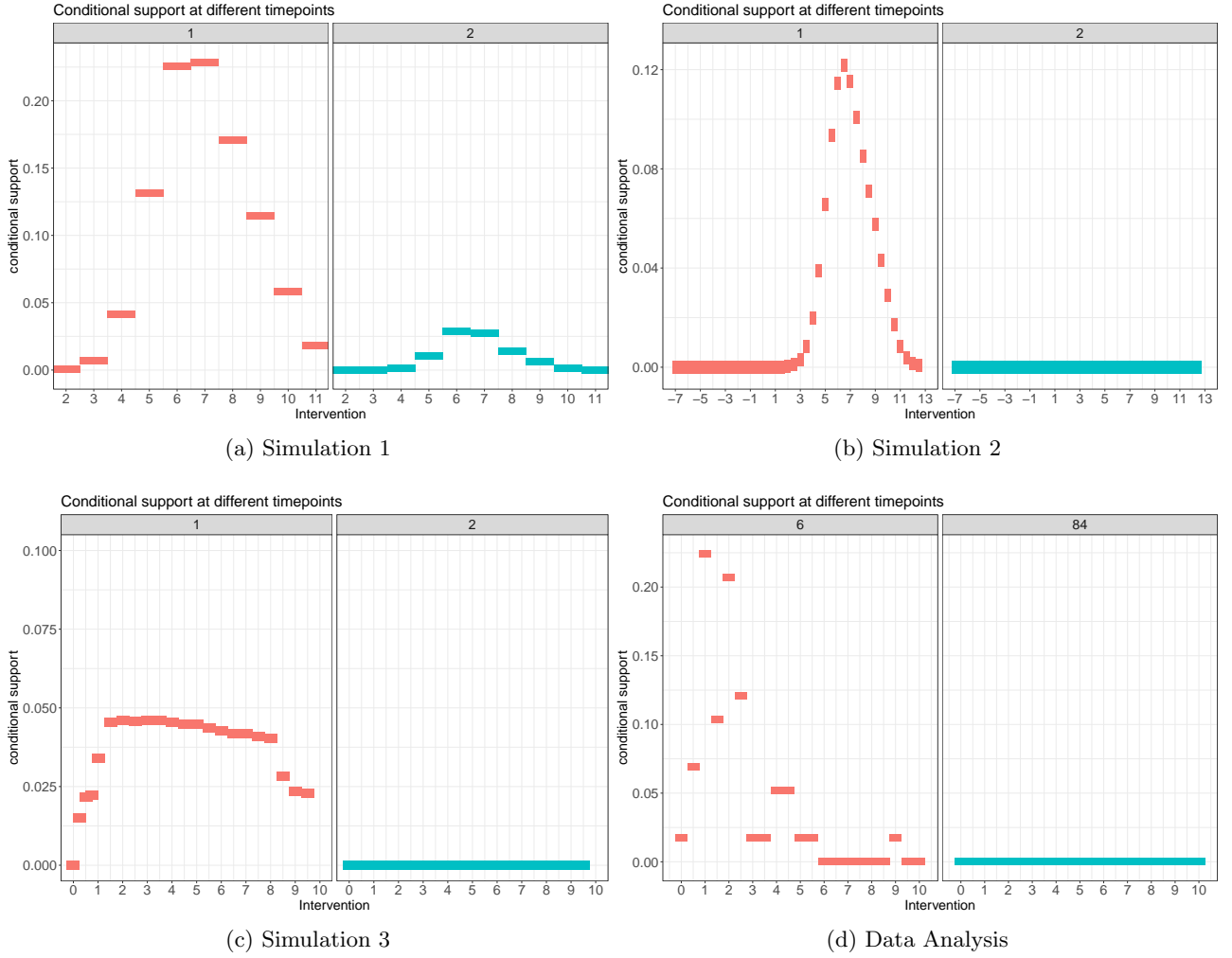


Figure 6: Conditional support for intervention strategies of interest, for both the simulation settings and the data analysis.

B Data-Generating Processes

B.1 DGP for Simulation 1

For $t = 0$:

$$\begin{aligned}
 L_0^1 &\sim B(p = 0.3) \\
 L_0^2 &\sim N(\mu = -1 + 2 \times L_0^1, \sigma = 1) \\
 A_0 &\sim N(\mu = 7 + L_0^1 + 0.7 \times L_0^2, \sigma = 1) \\
 Y_0 &\sim N(\mu = -1 + 0.5 \times A_0 + 0.5 \times L_0^2, \sigma = 1)
 \end{aligned}$$

For $t = 1, 2$:

$$\begin{aligned}
 L_t^1 &\sim B(p = 1/(1 + \exp(-(-4 + L_{t-1}^1 + 0.15 \times L_{t-1}^2 + 0.15 \times A_{t-1})))) \\
 L_t^2 &\sim N(\mu = 0.5 \times L_t^1 + 0.25 \times L_{t-1}^2 + 0.5 \times A_{t-1}, \sigma = 1) \\
 A_t &\sim N(\mu = A_{t-1} + L_t^1 - 0.1 \times L_t^2, \sigma = 0.5) \\
 Y_t &\sim N(\mu = -2 + 0.25 \times A_t - 0.2 \times L_t^1 + L_t^2, \sigma = 0.5)
 \end{aligned}$$

B.2 DGP for Simulation 2

For $t = 0$:

$$\begin{aligned} L_0^1 &\sim B(p = 0.3) \\ L_0^2 &\sim N(\mu = -1 + 2 \times L_0^1, \sigma = 1) \\ A_0 &\sim N(\mu = 7 + L_0^1 + 0.7 \times L_0^2, \sigma = 1) \\ Y_0 &\sim B(p = 1/(1 + \exp(-(-4 + 0.2 \times A_0 + 0.5 \times L_0^2)))) \end{aligned}$$

For $t = 1, 2, 3, 4$:

$$\begin{aligned} L_t^1 &\sim B(p = 1/(1 + \exp(-(-4 + L_{t-1}^1 + 0.15 \times L_{t-1}^2 + 0.15 \times A_{t-1})))) \\ L_t^2 &\sim N(\mu = 0.5 \times L_t^1 + 0.25 \times L_{t-1}^2 + 0.5 \times A_{t-1}, \sigma = 1) \\ A_t &\sim N(\mu = -2 + 0.5 \times A_{t-1} + 0.75 \times L_t^1 + 0.35 \times L_t^2, \sigma = 0.5) \\ C_t &\sim B(p = 1/(1 + \exp(-(-2 + 0.5 \times L_t^1 + 0.2 \times A_t)))) \\ Y_t &\sim B(p = 1/(1 + \exp(-(-4 + 0.2 \times A_t + 0.5 \times L_t^2)))) \end{aligned}$$

B.3 DGP for Simulation 3

Both baseline data ($t = 0$) and follow-up data ($t = 1, \dots, 4$) were created using structural equations using the *R*-package `simcausal`. The below listed distributions, listed in temporal order, describe the data-generating process. Our baseline data consists of sex, genotype, log(age), log(weight) and the respective Nucleoside Reverse Transcriptase Inhibitor (NRTI). Time-varying variables are co-morbidities (CM), dose, efavirenz mid-dose concentration (EFV), elevated viral load (= viral failure, VL) and adherence (measured through memory caps, MEMS), respectively. In addition to Bernoulli (B), Multinomial (MN) and Normal (N) distributions, we also use truncated normal distributions; they are denoted by $N_{[a,a_1,a_2,b,b_1,b_2]}$, where a and b are the truncation levels. Values which are smaller than a are replaced by a random draw from a $U(a_1, a_2)$ distribution and values greater than b are drawn from a $U(b_1, b_2)$ distribution, where U refers to a continuous uniform distribution. For the specified multinomial distributions, probabilities are normalized, if required, such that they add up to 1. The data-generating process reflects the following considerations: more complexity than the first two simulation settings in terms of distribution shape and variety, as well as non-linearities; similarity to the assumed DGP in the data analysis; generation of both areas of poor and good conditional intervention support, such that the proposed weighting scheme can be evaluated in all its breadth.

For $t = 0$:

$$\begin{aligned} \text{Sex}_0 &\sim B(p = 0.5) \\ \text{Genotype}_0 &\sim MN \left(\begin{array}{l} p1 = 1/(1 + \exp(-(-0.103 + I(\text{Sex}_0 = 1) \times 0.223 + I(\text{Sex}_0 = 0) \times 0.173))), \\ p2 = 1/(1 + \exp(-(-0.086 + I(\text{Sex}_0 = 1) \times 0.198 + I(\text{Sex}_0 = 0) \times 0.214))), \\ p3 = 1/(1 + \exp(-(-0.090 + I(\text{Sex}_0 = 1) \times 0.082 + I(\text{Sex}_0 = 0) \times 1.070))) \end{array} \right) \\ \text{Age}_0 &\sim N_{[0.693, 0.693, 1.2, 7, 2.7, 2.8]}(\mu = 1.501, \sigma = 0.369) \\ \text{Weight}_0 &\sim N_{[2.26, 2.26, 2.67, 3.37, 3.02, 3.37]}(\mu = (1.5 + 0.2 \times \text{Sex} + 0.774 \times \text{Age}) \times 0.94, \sigma = 0.369) \\ \text{NRTI}_0 &\sim MN \left(\begin{array}{l} p1 = 1/(1 + \exp(-(-0.006 + I(\text{Age}_0 > 1.4563) \times \text{Age}_0 \times 0.1735 + I(\text{Age}_0 \leq 1.4563) \times \text{Age}_0 \times 0.1570))), \\ p2 = 1/(1 + \exp(-(-0.006 + I(\text{Age}_0 > 1.4563) \times \text{Age}_0 \times 0.1735 + I(\text{Age}_0 \leq 1.4563) \times \text{Age}_0 \times 0.1570))), \\ p3 = 1/(1 + \exp(-(-0.006 + I(\text{Age}_0 > 1.4563) \times \text{Age}_0 \times 0.1570 + I(\text{Age}_0 \leq 1.4563) \times \text{Age}_0 \times 0.1818))) \end{array} \right) \\ \text{CM}_0 &\sim B(p = 0.15) \\ \text{Dose}_0 &\sim MN \left(\begin{array}{l} p1 = 1/(1 + \exp(-(-5 + \sqrt{(\text{Weight}_0)} \times 8 - \text{Age}_0 \times 10))), \\ p2 = 1/(1 + \exp(-(-4 + \sqrt{(\text{Weight}_0)} \times 8.768 - \text{Age}_0 \times 9.06))), \\ p3 = 1/(1 + \exp(-(-3 + \sqrt{(\text{Weight}_0)} \times 6.562 - \text{Age}_0 \times 8.325))), \\ p4 = 1 - (p1 + p2 + p3) \end{array} \right) \\ \text{EFV}_0 &\sim N_{[0.2032, 0.2032, 0.88, 21, 8.376, 21]}(\mu = -8 + \text{Age}_0 \times 0.1 + \text{Genotype}_0 \times 4.66 + \text{Dose}_0 \times 0.1 + I(\text{Genotype}_0 \leq 2) \times 2.66 + I(\text{Genotype}_0 = 3) \times 4.6, \sigma = 4.06) \\ \text{VL}_0 &\sim B(p = 1 - (1/(1 + \exp(-(-0.4 + 1.9 \times \sqrt{\text{EFV}_0})))) \end{aligned}$$

For $t \geq 1$:

$$\text{MEMS}_t \sim B(p = 1/(1 + \exp(-(-0.71 + \text{CM}_{t-1} \times 0.31 + \text{MEMS}_{t-1} \times I(t \geq 2) \times 0.31))))$$

$$\begin{aligned}
\text{Weight}_t &\sim N_{[2.26, 2.26, 2.473, 3.37, 3.23, 37]}(\mu = \text{Weight}_{t-1} \times 1.04 - 0.05 \times \text{I}(\text{CM}_{t-1} = 1), \sigma = 0.4) \\
\text{CM}_t &\sim \text{B}(p = 1 - (1/(1 + \exp(-0.5 \times \text{I}(\text{CM}_{t-1} = 1) + \text{Age}_0 \times 0.1 + \text{Weight}_{t-1} \times 0.1)))) \\
\text{Dose}_t &\sim \text{MN} \left(\begin{array}{l} p1 = (1/(1 + \exp(-(4 + \text{Dose}_{t-1} \times 0.5 + \sqrt{\text{Weight}_t} \times 4 - \text{Age}_0 \times 10))), \\ p2 = (1/(1 + \exp(-8 + \text{Dose}_{t-1} \times 0.5 + \sqrt{\text{Weight}_t} \times 8.568 - \text{Age}_0 \times 9.06))), \\ p3 = (1/(1 + \exp(-(20 + \text{Dose}_{t-1} \times 0.5 + \sqrt{\text{Weight}_t} \times 6.562 - \text{Age}_0 \times 18.325))), \\ p4 = 1 - (p1 + p2 + p3) \end{array} \right) \\
\text{EFV}_t &\sim N_{[0.2032, 0.2032, 0.88, 21.84, 8.37, 21.84]}(\mu = 0.1 \times \text{DOSE}_t + 0.1 \times \text{MEMS}_t + \text{I}(\text{Genotype}_0 \leq 2) \times 2.66 \\
&\quad + \text{I}(\text{Genotype}_0 = 3) \times 4.6, \sigma = 4.06) \\
\text{VL}_t &\sim \text{B}(p = 1 - (1/(1 + \exp(-1 - 0.6 \times \text{I}(t = 1) - 1.2 \times \text{I}(t = 4) + 0.1 \times \text{CM}_{t-1} + (2 - 0.2 \times \text{I}(t = 3)) \times \sqrt{\text{EFV}_t}))))
\end{aligned}$$

C More on the DAG

The measured efavirenz concentration depends on the following factors: the dose itself (which is recommended to be assigned based on the weight-bands), adherence (without regular drug intake, the concentration becomes lower), and the metabolism characterized in the gene CYP2B6, through the 516G and 983T polymorphisms [40]. Given the short half-life of the drug relative to the measurement interval, no arrow from EFV_t to EFV_{t+1} is required. Viral failure is essentially caused if there is not enough drug concentration in the body; and there might be interactions with co-morbidities and co-medications. Sometimes resistance could also lead to viral failure, but this point is less relevant in the data example. Note also that co-morbidities, which are reflected in the DAG, are less frequent in the given data analysis as trial inclusion criteria did not allow children with active infections, treated for tuberculosis and laboratory abnormalities to be enrolled into the study. Both weight and MEMS (=adherence) are assumed to be time-dependent confounders affected by prior treatments (=concentrations). Weight affects the concentration indirectly through the dosing, whereas adherence affects it directly. Adherence itself is affected by prior concentrations, as too high concentration values can cause nightmares and other central nervous system side effects, or strong discomfort, that might affect adherence patterns. Weight is affected from prior concentration trajectories through the pathway of viral load and co-morbidities. Finally, both weight and adherence affect viral outcomes not only through EFV concentrations, but potentially also through co-morbidities such as malnutrition, pneumonia and others.